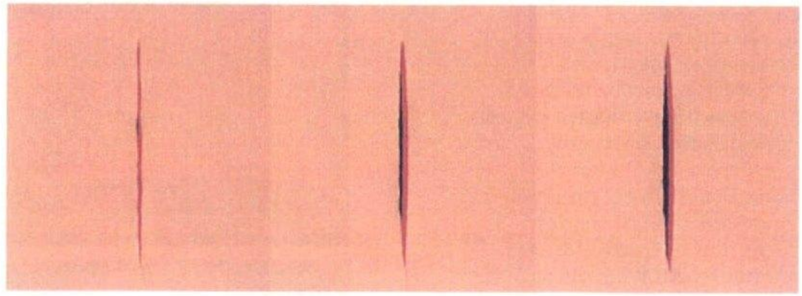

Fig. 10. Example of simulated incision in case of 2, 4, and 6% tension

around incision become the modeling targets and 8.4 s is required for constructing the stiffness matrix. The localization scheme reduces modeling cost and gives valid estimation based on physical characteristics of soft tissues. This approach allows the user to input the incision interactively and to simulate accurate FEM-based deformation after several seconds.

Next, we confirm quality and performance of FEM-based deformation of incision using the proposed virtual hook model with four or eight control points. As shown in Fig. 11, deformed incision depends on the number of control points. In case of (b), smooth incision is provided. However, even in the eight control point case, the shape of incision seems not to follow the hook shape. Since the control points become boundary condition to the FEM model, the deformation results are influenced by their placement on the model. Although more accurate simulation results are obtained using a detailed hook model, increase of control points becomes drawback to real-time deformation. In case of Fig. 11, the calculation time per one frame was 1.91 and 7.54 ms, respectively. Because large incision is estimated to be at most 40 cm in surgery, this quality and performance are valid for specific planning use.

Clinical trial

Thirdly, field trials were given with four cardiovascular surgeons using the developed system and clinical CT dataset. Figure 12 illustrates a hybrid virtual body reconstructed from an aortic arch aneurysm case. The chest wall consists of tetrahedral mesh and other parts like bone, aorta, and heart are voxels.

Table 1 Comparison of mesh modification techniques

	Increase of elements (Average)	Subdivision pattern
Model 1 (General)	16	1
Model 2	8.6	5
Model 3	5.6	11
Model 4 (Adaptive)	4.8	2

2D CT images were first presented to the surgeons. The surgeons discussed the best approach by the conventional way used in the current preoperative planning. Three standard approaches: Median incision approach, intercostal incision approach, and distal incision approach were considered. Consequently, two surgeons selected median incision approach and the other surgeons selected intercostal approach.

To support discussion for these two approaches, the developed planning system was used. The surgeons rehearsed procedures in approaching the target aneurysm region. Cutting line was given on the 3D virtual patient model and incision was opened interactively. Figure 12(a) illustrates the planned median incision and the estimated surgical field. The simulation results show that median incision approach is easy to palpate aortic arch around the aneurysm for grasping sclerosis status. However, a part of distal aneurysm cannot be observed. Thus, the surgeons confirmed several key points that require careful treatment in surgery. Figure 12(b) shows the intercostal incision approach and the estimated surgical field. Although this approach enables surgeons to recognize whole shape of aneurysm, it also suggests a possibility of removing the costal. The surgeons compared the two approaches using simulation results and determined intercostal incision approach is better based on the relationship of the aneurism region and the surgical field.

We also gave another experiment, which is totally virtual preoperative planning of minimally invasive direct coronary artery bypass grafting (MIDCAB). Surgeons gave

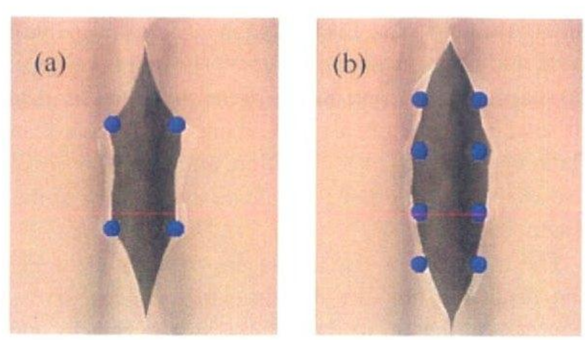

Fig. 11 Deformation of incision using four and eight control points

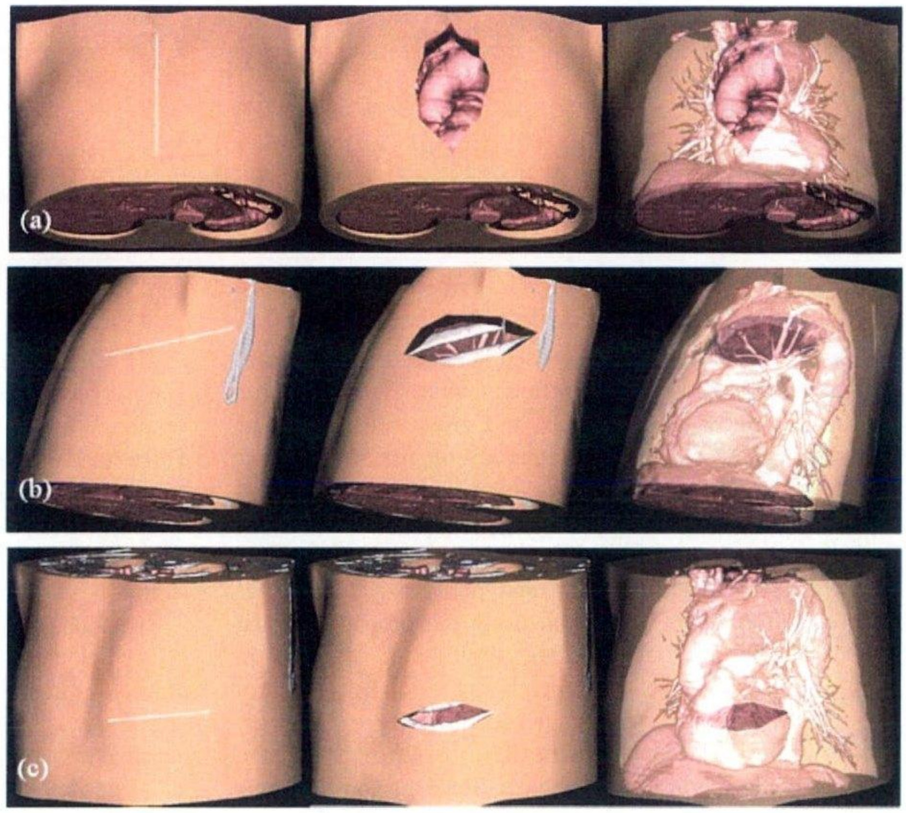

Fig. 12 Results of strategic approach planning of aorta aneurysm surgery. (a) Rehearsing midline incision approach and estimated surgical field. Aneurysm is partly observed. (b) Intercostal incision approach. Aneurysm is grasped without bone. (c) Surgical approach selected in virtual MIDCAB planning. Anastomotic point is located at the center of surgical field

cutting lines for approaching the region and the target point where an internal artery is connected was visualized on the 3D patient model. Four different approaches were proposed (Fig. 12(c)). The surgeons carefully observed relationship of the target point and incision and selected one best approach. The target point of the selected approach is located in the center of the surgical field. The surgeons used this factor to determine the best approach and adjusted incision by rotating or enlarging the virtual body. These results show the reconstructed surgical field is efficient to discuss fine adjustment of incision in minimally invasive surgery.

Characteristic evaluation

Finally, characteristic evaluation was given based on the results of the field trials. Each surgeon marked one to five points to six questions on a questionnaire. The first three questions: 3D shape, location, and quality of the simulated surgical field are selected as functional requirements for strategic planning. Planning effect, crisis recognition, and overall necessity are also examined in order to evaluate availability of the total system.

The averages of the points are designated in Fig. 13. The results assure that the simulated images of the system are sufficient to grasp 3D shape and location of the organs in the surgical filed. However, as a result of discussion with the surgeons, they require more detailed image of other minute organs and tissues such as coronaries and nerves. From this viewpoint, they commented the increase of overall applicability of the system required to improve visual quality of anatomical information.

Discussion

The result of evaluation demonstrates that the developed system simulates procedures for setting up surgical fields and efficiently supports planning of surgical approach. On the other hand, several issues on the system are also revealed.

In this paper, uniform value is used for elastic parameters (e.g., springs and their tension) of the model. For improving reality of interactive cutting, detailed parameter setting is required considering topology of the mesh. However, resetting all parameters of particle systems is time-consuming task and is not always necessary because deformation of incision is still small during cutting manipulation. After cutting operation, accurate deformation of incision is provided based on finite element formulation.

Although the developed framework employs a linear finite element model for performing accurate simulation results, deformation of incision by surgical hooks become large especially in open surgery. In this case, the linear elastic model

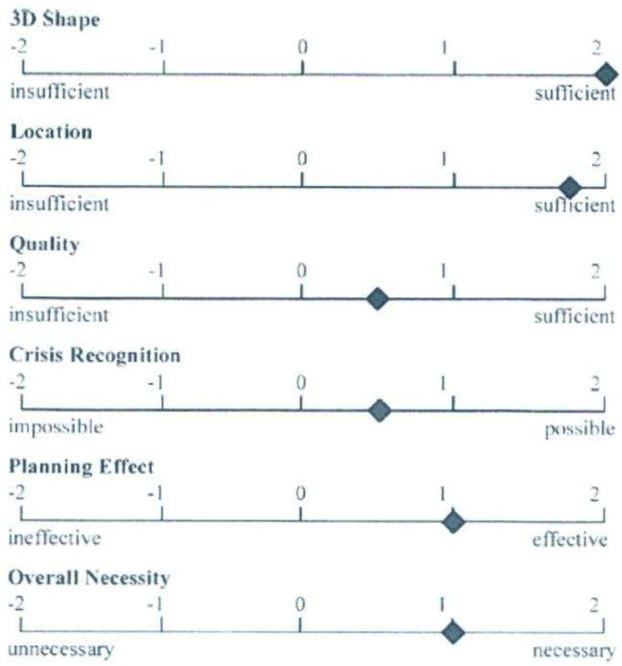

Fig. 13 Characteristic evaluation of the strategic planning system

is not sufficient due to non-linear anisotropic characteristics of soft tissues. In order to simulate such physical behavior, several methods [29] have been reported.

Regarding functions of the planning system, several procedures (e.g., ablation) in setting up surgical fields are skipped. This assumption is effective under the condition that the target organ does not change its position drastically like in minimally invasive surgery or in some cases of thoracic surgery. To improve applicability of the system, influence of both organ–organ interaction and ablation process should be handled.

Consequently, our future direction is to improve quality and performance of the physics-based framework and to examine validation of the system through clinical trials.

Conclusion

This paper first proposes an adaptive physics-based framework that simulates both interactive cutting and accurate deformation on reconstructed virtual bodies.

The framework modifies tetrahedral mesh via cutting manipulation, and then constructs stiffness matrix required for finite element-based simulation. This adaptive subdivision is simple for implementation and efficiently reduces increase of elements. In addition, the fast computation scheme provides valid solution for simulating widespread soft tissue cutting interactively.

A deformable incision model using a virtual hook enables widespread deformation in real time, and simulates construction of estimated surgical field. Improving simulation quality using online finite element modeling is effective to achieve realistic estimation of intra-operative physical behavior for preoperative planning.

Using the proposed methods, we developed a strategic planning system that supports decision of surgical approach, and applied measured clinical dataset of an aortic aneurysm case. Some experiments and usability tests made it clear that the system contributes to grasping 3D shape and location of the target organs. These results confirm that the developed system efficiently supports detailed planning of patient-specific surgical approaches.

Acknowledgments This research is supported by Grant-in-Aid for Scientific Research (S) (16100001) and Young Scientists (A) (16680024) from The Ministry of Education, Culture, Sports, Science and Technology, Japan.

References

1. Gorman, P. J., Meier, A. H., and Krummel, M., Computer-assisted training and learning in surgery. *Comput. Aided Surg.* 5:120–127, 2000.
2. Gross, M., Graphics in medicine: From visualization to surgery simulation. *ACM Comput. Graph.* 32:53–56, 1998.
3. Hohne, K. H., Pflesser, B., Pommert, A., Riemer, M., Schiemann, T. H., Schubert, R., and Tiede, U., A new representation of knowledge concerning human anatomy and function. *Nat. Med.* 1(6):506–511, 1995.
4. Koch, R. M., Gross, M. H., Carls, F. R., Bren, D. F., Fankhauser, G., and Parish, Y. I. H., Simulating facial surgery using finite element models. *ACM SIGGRAPH* 421–428, 1996.
5. Xia, J., James, X., Horace, H. S. I., Nabil, S., Helena, T. F. W., Jaime, G., Dongfeng, W., Richie, W. K. Y., Christy, S. B. K., and Henk, T., Three- dimentional virtual-reality surgical planning and soft-tissue prediction for orthognathic surgery. *IEEE Trans. Inform. Technol. Biomed.* 5(2):97–107, 2001.
6. Preim, B., Spindler, W., Oldhafer, K. J., and Peitgen, H. O., 3D-Interaction techniques for planning of oncologic soft tissue operations. *Proc. Graph. Interface* 2001.
7. Ehrhardt, J., Handels, H., Malina, T., Strathmann, B., Plotz, W., and Poppl, S. J., Atlas-based segmentation of bone structures to support the virtual planning of hip operations. *Int. J. Med. Inform.* 64:439–447, 2001.
8. Omoto, R., *Minimally Invasive Cardiac Simulation*, Shindan to Chiryo Inc., Japan, 1999.
9. Basdogan, C., Ho, C. H., and Srinivasan, M. A., Simulation of tissue cutting and bleeding for laparoscopic surgery using auxiliary surfaces. *Med. Meets Virtual Real.* 38–44, 1999.
10. Bruyns, C., Senger, S., Interactive cutting of 3D surface meshes. *Comput. Graph.* 25:635–642, 2001.
11. Reining, K. D., Rush, C. G., Pelster, H. L., Spitzerm, V. M., and Heath, J. A., Real-time visually and haptically accurate surgical simulation. *Health Care Inform. Age* 542–546, 1996.
12. Pflesser, B., Petersik, A., Tiede, U., Hohne, K. H., and Leuwer, R., Volume cutting for virtual petrous bone surgery. *Comput. Aided Surg.* 7(4):74–83, 2002.
13. Bielser, D., and Gross, M. H., Interactive simulation of surgical cuts. *Pac. Graph.* 116–125, 2000.

14. Ganovelli, F., Cignoni, P., Montani, C., and Scopigno, R., Enabling cuts on multiresolution representation. *Vis. Comput.* 17:274–286, 2001.
15. Mor, A., Progressive cutting with minimal new element creation of soft tissue models for interactive surgical simulation. Doctoral Dissertation, Tech. Report CMU-RI-TR-01-29, Robotics Institute, 2001.
16. Braff, D., and Witkin, A., Physically based modeling: Principles and practice. ACM SIGGRAPH97 Course Notes, 1997.
17. Gibson, S., and Mirtich, B., A survey of deformable modeling in computer graphics. *MERL Tech. Rep.*, TR97-19, 1997.
18. Nedel, L. P., and Thalmann, D., Real time muscle deformations using mass-spring systems. *Comput. Graph. Int.* 156–165, 1998.
19. Kuhnapfel, U., Cakmak, H. K., and Mass, H., Endoscopic surgery training using virtual reality and deformable tissue simulation. *Comput. Graph.* 24(5):671–682, 2000.
20. Bro-Nielsen, M., and Cotin, S., Real-time volumetric deformable models for surgery simulation using finite elements and condensation. *Eurograph. Comput. Graph. Forum* 15(3):57–66, 1996.
21. Hirota, K., and Kaneko, T., A method of representing soft tissue object in virtual environment. *Trans. IPSJ* 39(12):3261–3268, 1998.
22. Cotin, S., Herve, D., and Ayache, N., A hybrid elastic model for real-time cutting, deformations, and force feedback for surgery training and system. *Vis. Comput.* 16:437–452, 2000.
23. Nienhuys, H. W., and Stappen, A. F., A surgery simulation supporting cuts and finite element deformation. *MICCAI* 153–160, 2001.
24. Nakao, M., Kuroda, T., Oyama, H., Komori, M., Matsuda, T., and Takahashi, T., Planning and training of minimally invasive surgery by integrating soft tissue cuts with surgical views reproduction. *CARS* 13–18, 2002.
25. Nakao, M., Kuroda, T., Oyama, H., Komori, M., Matsuda, T., and Takahashi, T., Combining volumetric soft tissue cuts for interventional surgery simulation. *MICCAI* 178–185, 2002.
26. Berkley, J., Weghorst, S., Gladstone, H., Gaugi, G., Berg, D., and Ganter, M., Banded matrix approach to finite element modeling for soft tissue simulation. *Virtual Real. Res. Dev. Appl.* 4:203–212, 1999.
27. Ruspini, D., Kolarov, K., and Khatib, O., The haptic display of complex graphical environments. *ACM SIGGRAPH* 345–52, 1997.
28. Nakao, M., Kuroda, T., and Oyama, H., An input method of surgical plans by mouse manipulation. *Hum. Interface Symp.* 301–304, 2002.
29. Picinbono, G., Delingette, F., and Ayache, N., Non-linear anisotropic elasticity for real-time surgical simulation. *INRIA Yearly Activity Rep.* 2000.

Transferring Bioelasticity Knowledge through Haptic Interaction

Megumi Nakao and Kotaro Minato
Nara Institute of Science and Technology

Tomohiro Kuroda
Kyoto University Hospital

Masaru Komori
Shiga University of Medical Science

Hiroshi Oyama
University of Tokyo

Takashi Takahashi
Kyoto College of Medical Technology

This study establishes a practical environment for transferring knowledge on bioelasticity between expert and trainee medical practitioners. Through haptic interaction with a deformable virtual anatomical model, experts set the model's elasticity conditions by simulating a surgical procedure. Trainees experience the elasticity by attempting the same surgical manipulation.

Knowledge of soft-tissue bioelasticity is essential to medical practitioners in making a successful diagnosis and skillfully carrying out surgical procedures, such as palpation or handling surgical tools. Intraoperative palpation, for example, lets clinical medical practitioners determine the medical status of the body's organs, so it's essential that practitioners understand soft tissue's physical characteristics. Currently, general bioelasticity training is conducted in a "learn by doing" approach during daily medical work. This approach, the traditional style of clinical education, offers few chances for practice in clinical fields. Consequently, it's difficult for students to gain systematic experience in dealing with a wide variety of diseases or rare cases.

In this article, we describe how we constructed haptic media to represent the specific physical behavior of a beating aorta for instructing intraoperative palpation in cardiovascular surgery. We analyze the results of a communication sequence during a user study that involved skilled cardiovascular surgeons and students who trained on haptic interaction using our virtual, deformable models. The study tested this method's effectiveness in communicating both key elasticity properties and the means of manipulation required to master palpation. It's difficult to determine an aorta's bioelasticity, especially in cases such as sclerosis. Therefore, both the approach we created and the quantified knowledge gained during our study will be useful indices for the future development of haptically valid anatomical models.

We chose this area to investigate because currently, there's no training environment provided for intraoperative palpation despite its being a basic technique that all cardiovascular surgeons need to master. Another reason is that the aorta palpation procedure is simple and is performed with a simple push of a finger. Because current force-feedback devices, such as SensAble Technologies' Phantom (http://www.sensable.com), ably support the push operation, the only additional requirement for creating a realistic interaction environment is a valid physics-based aorta model.

Background: Surgical training methods

Virtual reality (VR)-based surgical simulators[1-7] have emerged as possible practical environments for residents to attempt repetitive training in surgical procedures. Physics-based models have been developed for simulating visual and haptic feedback of virtual organ manipulation.[8-15] Recent studies report that simulator-based training helps improve the results of actual surgery.[16,17]

Some of these haptic simulators, targeted specifically at palpation training, are designed to support bioelasticity knowledge acquisition.[4,5] In fact, we too have developed palpation simulators,[6,7] which concentrate on modeling beating behavior and organ–organ interaction in human bodies. In general, these simulators require more accurate haptic displays than the training simulators used in tool manipulation, such as suturing.[2,3,13]

More work, however, remains to be done to advance palpation simulators so they can be used effectively in training. The main obstacle lies in developing valid anatomical models because of the difficulty in accurately specifying organs' elasticity. Output from simulations varies accord-

1070-986X/06/$20.00 © 2006 IEEE

Published by the IEEE Computer Society

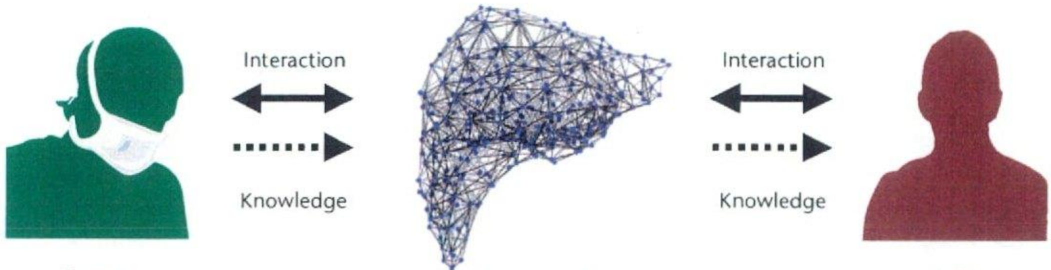

Figure 1. Basic concept. Elastic models support communication between experts and trainees as deformable media. Experts transfer their elasticity knowledge onto the models and trainees study the elastic behavior through haptic interaction.

ing to physical parameters and the complexity of the virtual organs that are being manipulated. Techniques for modeling patient-specific elasticity haven't yet been established; consequently, it's difficult to create accurate models for diseased organs. In addition, the effectiveness of training using haptic simulators must be further evaluated so that researchers can understand and improve simulator performance.

On the other hand, instruction by skilled medical practitioners has traditionally played a large role in the education of patient-specific elasticity. In practical situations, experts sometimes communicate images that are difficult for residents to conceptualize by referring to similar, known elastic objects. This approach is an accepted method of teaching, but verbal communication alone, without hands-on experience, isn't sufficient for effectively transferring knowledge on tissue elasticity. Therefore, an optimized education process requires a combined approach using both simulation and skilled instruction. If an expert's knowledge on bioelasticity could be efficiently transferred to trainees via a computer-assisted environment, trainees would learn key elasticity skills, including those needed for disease and rare-case scenarios.

Researchers have made some headway in developing haptic communication between experts and trainees. Haptic teaching systems developed in other fields focus mainly on tool manipulation[18,19] and are used to teach trajectory and applied force, especially in the field of handwriting. Satoshi Saga and colleagues[19] have proposed a haptic video system, which replays the force history acquired from an expert's manipulation. These approaches support the instruction of tool manipulation rather than provide a simulation environment where objects are manipulated. In manipulating elastic objects, such as during a surgical procedure, a surgeon feels reaction force other than that resulting from the tool's position. Consequently, a surgeon's education in physical behavior of elastic objects must include both haptic interaction and physical modeling of the object under manipulation.

In our study, we aimed to establish a communication support environment for transferring knowledge on bioelasticity using virtual anatomical models. Figure 1 shows the basic concept. We propose an interactive system that lets skilled medical staff instruct residents or medical students in organ bioelasticity by haptic interaction with the models. In our deformable media approach, virtual models are used to transfer elastic information from experts to trainees. The elastic information is stored quantitatively as part of the model's physical parameters. In a simple process, experts set up the model according to their experience, and trainees learn how to perceive the elastic information by attempting surgical procedures on the same model.

Supporting communication on bioelasticity

Medical practitioners generally learn objects' elasticity through attempting to recognize their physical behavior by conducting haptic interaction maneuvers, such as direct hand manipulation or varying the manner of contact. Practitioners also learn bioelasticity properties associated with specific diseases by touching and manipulating tumors in daily medical work.

Basic principles

To advance current training methods and techniques, practitioners require a platform on which medical procedures can be practiced. This platform—haptic media—should serve to let experts share their knowledge and trainees conduct self-study in the virtual space. Here, we outline the basic design, and the two primary tasks, of our proposed environment:

1. *Expert sets virtual model elasticity.* Experts simulate medical procedures on the virtual

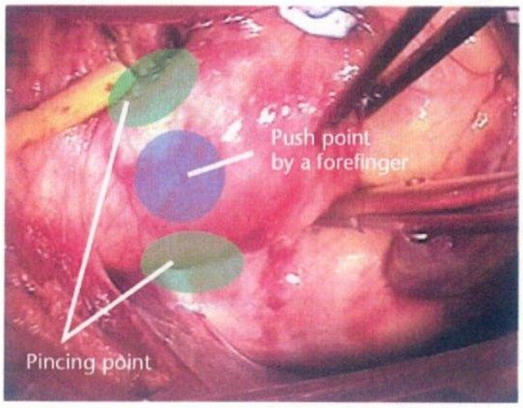

Figure 2. Intraoperative palpation in total aortic arch replacement surgery. Surgeons push or pinch the aorta's surface wth one or two fingers to identify the sclerotic region for diagnosis and overall strategy planning.

model. The feedback reaction force and deformation help the expert perceive the model's elasticity and compare with previous experience. If the elasticity differs from the expert's expectation, the expert changes the model's physical parameters. When the model's physical behavior matches the expert's expectation, the elastic parameters are stored, which completes this task.

2. *Trainee learns virtual model elasticity.* In this task, trainees experience the model's elasticity by repeatedly performing the same manipulation that the experts carried out in the first task. Over time—which might involve a trainee's conducting the same procedure once every few days—the trainee acquires a stable perception of different conditions, and recognizes the elasticity relating to a specific situation.

Virtual aorta palpation system design

For discussion purposes, we've considered a total aortic arch-replacement surgery. In such a surgery, surgeons must perform intraoperative palpation of the aorta to establish the tissues' elasticity. Surgeons do so because they need to identify the sclerotic region to determine the overall surgical strategy required to deal with the tumors (see Figure 2). Because the nature of the sclerotic region cannot be ascertained from visual information, such as texture and 3D shape alone, surgeons—using one or two fingers—push or pinch several points of the aorta.

To provide practitioners with an interactive environment enabling them to rehearse realistic palpation procedures, we first need a clear description of how interaction with the virtual model should occur. Furthermore, it's essential to engineer realistic visual and haptic feedback. Specifically, the aorta model must aptly simulate both autonomous beating and volumetric distribution of elasticity equivalent to that of the sclerotic status of real-life tissue. Additionally, to accurately model the surgeon's manner of palpation, the haptic interface should support both one- and two-finger manipulation. Finally, the interactive modeling interface should allow surgeons to modify physical parameters based on their empirical bioelasticity knowledge.

On the basis of these requirements and additional discussions with cardiovascular surgeons, we've designed a virtual aorta palpation system (see Figure 3). The system visualizes a 3D aortic arch model as a polygonal object in the virtual space. Users control two sphere-shaped manipulators via two Phantom haptic devices—model Premium 1.5. The manipulators represent the 3D positions of a user's thumb and index finger, respectively. The Phantom's collision detection algorithm responds to any interaction between the manipulators and the model, while the physics-based simulation algorithm calculates the reaction force and deformation using the contact points and manipulators' current positions. The Phantom device conveys the calculated reaction force to the user and displays the deformation result on the screen as a transformation of the 3D model. The Phantom haptic device also lets surgeons interactively update the model's elasticity and boundary conditions when the physical behavior differs from the surgeons' expectations. We provide a graphical user interface that supports elastic modeling and manages given physical parameters.

To simulate the physical behavior of a beating aorta while maintaining a haptic-compatible refresh rate, we propose new finite-element-based computation methods. Although many studies have concentrated on developing various kinds of physics-based models,[8-15] the finite element method (FEM) is known to be the most accurate computational model for simulating the biomechanical behavior of elastic soft tissues. Although FEM-based simulation provides accurate and stable deformation, however, it carries a high calculation cost. To allow real-time interaction with a volumetric-deformable object, Morten Bro-Nielsen and Stephane Cotin have proposed a condensation technique.[9] This technique reduces the size of a stiffness matrix in the preprocessing stage and performs real-time simulation for detailed objects. More recently, Koichi Hirota and Toyohisa Kaneko have achieved fast computation of reaction force by using an efficient translation of a matrix calculation.[14]

Although most previous studies didn't try to simulate dynamic behavior like pulsation or beating status, our previous study detailed the 3D anatomical shapes and approximate time series pressure required to realistically represent the haptic feedback of heartbeats.[6] In the study, we've used these features to create haptic-deformable media to represent a beating aorta's dynamic behavior during cardiovascular surgery. Our proposed FEM-based computation methods then calculate the reaction force and biomechanical deformation that reflects the internal pressure induced by the user's manipulation.

Physics-based modeling of a beating aorta

Physics-based simulation requires a 3D shape with elastic information of the target organ.

3D shape and elasticity modeling

To construct our virtual aorta model, we acquired images of patients' aortas from computerized tomography or magnetic resonance imaging techniques. We extracted a 3D region of the aorta from voxels and divided them into finite tetrahedra. Each tetrahedron represented a part of the 3D region of the aorta and also its particular physical parameters: Young's modulus and Poisson's ratio, which are measures of elasticity. We used the volumetric grid topology and physical parameters to calculate a stiffness matrix, enabling finite-element-based simulation. We categorized all vertices, based on three different boundary conditions, into fixed vertices, internal wall vertices, and other free vertices. Fixed vertices represented tissue that connects or contacts other organs. Internal wall vertices represented the aorta's beating, holding dynamic force by a time series of blood pressure data. We represented the condition of arterial sclerosis by setting a high Young's modulus to the desired region.

We created a virtual 3D shape of a normal aortic arch from the Visible Human Male data set.[20] Using Mercury Computer Systems' Amira 3.1 modeling software (http://www.amiravis.com), we reconstructed the aorta surface and generated tetrahedral grids. Figure 4 illustrates the constructed aortic arch model. The total number of the vertices was 1,651. The edge vertices of the 3D model, which simulated connection to the heart and other vessels, were defined as fixed because these areas didn't move in actual palpation. Each vertex was represented as a small sphere colored according to its boundary condition, shown in Figure 4.

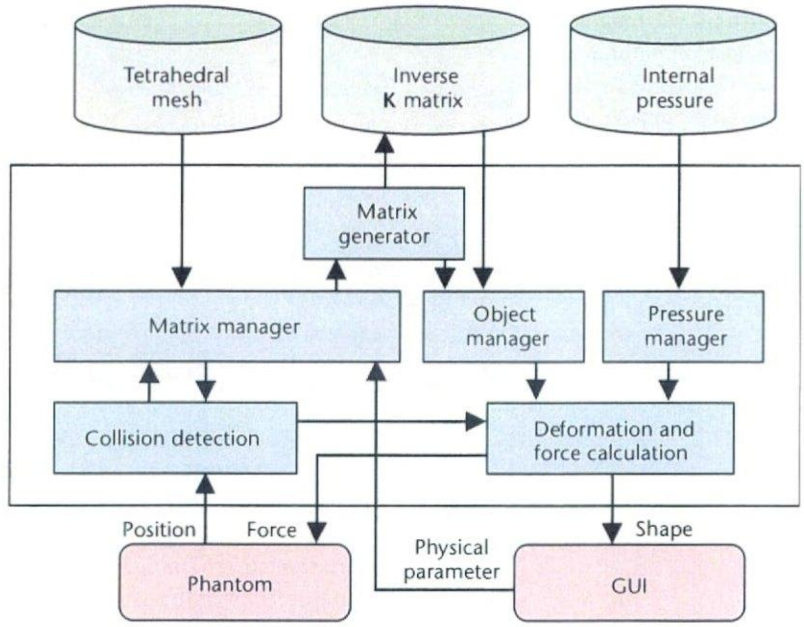

Figure 3. Overall framework for the simulation system developed for instructing palpation of the aorta. Surgeons and residents used this system to rehearse realistic palpation procedures on the virtual aorta model. Skilled surgeons conveyed their bioelasticity knowledge by modifying the model elasticity.

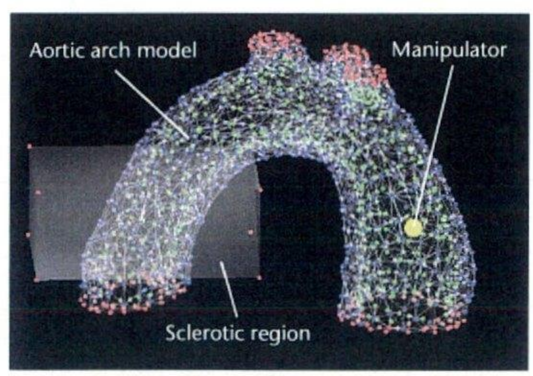

Figure 4. The aortic arch model. The 3D shape was acquired from the Visible Human Male data set. A high Young's modulus was given to tetrahedral elements in the sclerotic region using a 3D bounding box. The colors of vertices represented boundary conditions. Red vertices were "fixed," green vertices were "internal wall," and blue vertices were "free" for deformation.

The system we developed also provided an elastic modeling interface to support flexible parameter setting by skilled surgeons. The view of the virtual space contained a 3D bounding box (see Figure 4) whose shape and 3D position were controlled interactively using a slider bar and edit box in the graphical user interface. We also prepared several shape templates such as spheres and cubes. This interface let surgeons modify the model elasticity and boundary conditions as needed. Following this interactive elasticity modeling, the system automatically updated the stiffness matrix by running matrix generation algorithms.

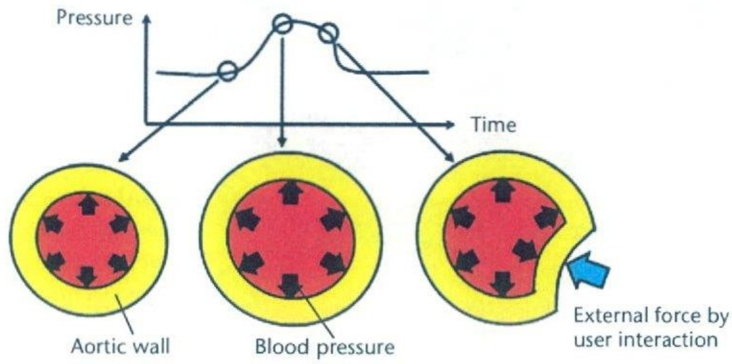

(a) (b) (c)

Figure 5. FEM-based computation model for a beating aorta: (a) 3D shape; (b) aorta expansion after higher pressure exerted; and (c) the result of external force applied.

Haptic interaction

The collision-detection algorithm, in conjunction with physics-based simulation, enabled virtual palpation to be performed on the aorta model. The algorithm handled the intersection between the model's fingertip manipulators and the tetrahedral grids, for which we employed proxy-based haptic rendering methods.[21,22] The algorithm was based on point-polygon collision detection, which, despite being a simplification of a real aorta, was sufficient to handle the basic interaction of a surgeon's fingertips touching the aortic wall in real surgery. The main challenge of this study was to simulate and describe interaction with a deformable object that's subject to autonomous beating.

Figure 5 outlines the basis of our haptic interaction model for aorta palpation. A 2D cylinder cross-section approximately illustrates the aortic wall. When blood pressure was applied to the wall (depicted in Figure 5a), the FEM-based simulation responded by expanding the 3D shape. The higher the pressure applied, the larger the expansion, as Figure 5b shows. The system provided simulation results at discrete time steps, effectively modeling the aorta wall's autonomous beating. In addition, when an external force initiated a small displacement in the aorta model, the reaction force was calculated and conveyed to the user's fingertips via the Phantom devices, indicated in Figure 5c.

Cardiovascular surgeons reported that, during a palpation procedure, they avoid pinching the aortic wall too hard to avoid damaging soft tissues and to minimize the aorta's deformation. Therefore, our proposed model assumed that internal blood pressure wasn't affected by surgical palpation, evidence that linear finite element models were a good approximation for real-life aorta palpation.

FEM-based computation

We based our calculation method—to simulate the reaction force and deformation of a beating aorta—on linear elastic theory. Assuming that the internal force is in equilibrium at each discrete time step, the relationship between external force and displacement on an elastic object is defined by $f = \mathbf{K}u$ where, on all vertices, u is displacement and f is external force, including blood pressure. $\mathbf{K}$ denotes the stiffness matrix of the object constructed by grid topology and physical parameters (Young's modulus and Poisson ratio). The $\mathbf{K}$ matrix can be efficiently reduced by condensation[9] and elimination of the fixed vertices in the preprocessing stage. This expression is simplified to $u = \mathbf{L}f$ using the condensed inverse stiffness matrix $\mathbf{L}$, which defines the physical relationship between the external force f and the displacement u on the surface vertices.

To represent autonomous beating and to simulate the physical behavior of the user's interaction, we divided the surface vertices into three groups: contacted vertices, internal wall vertices, and other free vertices. Contacted vertices are directly displaced by the user's manipulation. Internal wall vertices are affected by the time series of blood pressure. Equation 1 expands $u = \mathbf{L}f$ by using the initial letters of categorized vertices to represent the coefficients of the matrices.

$$\begin{pmatrix} u_i \\ u_o \\ u_c \end{pmatrix} = \begin{pmatrix} \mathbf{L}_{ii} & \mathbf{L}_{io} & \mathbf{L}_{ic} \\ \mathbf{L}_{oi} & \mathbf{L}_{oo} & \mathbf{L}_{oc} \\ \mathbf{L}_{ci} & \mathbf{L}_{co} & \mathbf{L}_{cc} \end{pmatrix} \begin{pmatrix} f_i \\ f_o \\ f_c \end{pmatrix} \tag{1}$$

where f_i denotes blood pressure that's applied to the internal wall vertices and u_c is displacement of the contacted vertex manipulated through the Phantom haptic device. Considering that f_o is constant zero, the relationship between u_c, f_i, and f_c is described as $u_c = \mathbf{L}_{ci}f_i + \mathbf{L}_{cc}f_c$. Consequently, f_c is given as $f_c = \mathbf{L}_{cc}^{-1}(u_c - \mathbf{L}_{ci}f_i)$.

Accordingly, f_c is external force on the contacted vertex, and $-f_c$ is reaction force conveyed to the user. Note that we can obtain $\mathbf{L}_{cc}$ and $\mathbf{L}_{ci}$ by precomputation because both are defined by Young's modulus and Poisson's ratio. We calculate $\mathbf{L}_{cc}$ and $\mathbf{L}_{ci}$ for all free vertices and perform a refresh rate of more than 1,000 Hz to maintain stable force feedback. The dynamic transition of f_c at discrete time steps lets us present haptic feedback of the beating aorta under the effects of time series blood pressure. Applying f_c to Equation 1 provides the displacement u_o on other free vertices.

Evaluation and user study

In this section, we describe the virtual palpation system's operation, example results, and outputs. We then present the design of studies that evaluate the effectiveness of our system in supporting communication on bioelasticity.

System verification

We processed the computation algorithms on a standard PC with a Pentium 4 2.4-GHz CPU and 1,024 Mbytes of memory. We optimized the matrix calculation on the CPU with Intel's Math Kernel Library.

Our first step was to confirm the visual and haptic quality and performance of the developed system with cardiovascular surgeons. In this experiment, we set Young's modulus of the normal model to 1.0 megapascal (MPa), that of the sclerotic model to 3.0 MPa, and the Poisson's ratio to 0.48, based on the measured data for a normal aortic wall that we'd obtained previously.[23] Later, we explain how we tested the model's physical characteristics, compared to the empirical knowledge of skilled cardiovascular surgeons.

Figure 6 shows how the user interacted with the virtual system and gives an example of the deformation that occurred in the virtual aorta following pinching with two fingers. The user touched two manipulators in real space with the tips of the Phantom devices that were worn on the fingertips (bottom-left image). These manipulators translated the position of the fingertips to the model aorta in the virtual space. In Figure 6, we highlight the virtual position of the fingertips (top-left image) that corresponded to the fingertips' real position (bottom-left image).

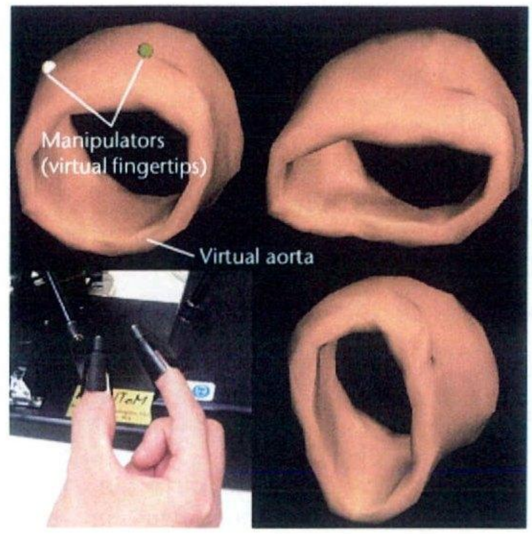

Figure 6. Real-time deformation in palpating the virtual aorta. Two manipulators controlled by two SensAble Technologies' Phantom haptic devices enable users to pinch the model interactively.

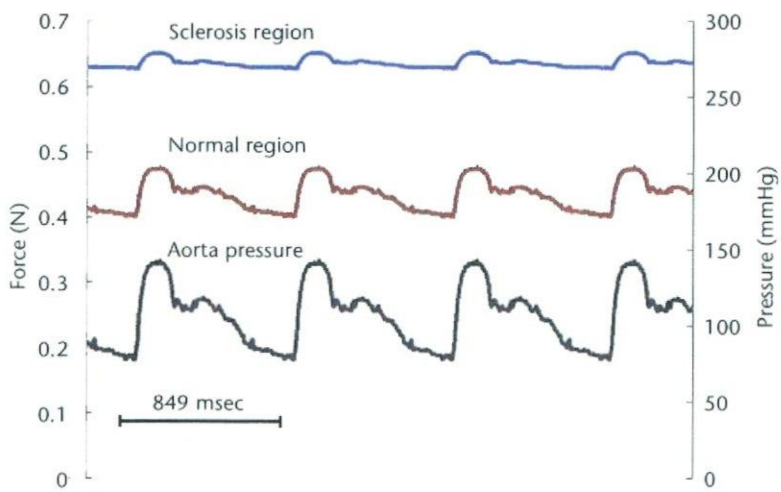

Figure 7. Reaction force in pushing normal/sclerotic region on a virtual aorta sclerotic model. This simulation result demonstrated that the sclerotic part did not reproduce the pulse with as great a magnitude as normal tissue.

Next, we tested the accuracy of the model in simulating both normal and sclerotic aorta conditions. The proposed FEM-based model simulated reaction force and deformation for an aorta subjected to time series pressure. Figure 7 shows the relationship between a dynamic transition of the reaction force and the applied time series blood pressure when the aorta wall was subjected to a specific displacement by the fingers. We programmed two regions of the virtual aorta, each with a different state (normal and sclerotic). The two different regions showed different absolute values of reaction force and beating status for the same given displacement. The sclerotic part did not reproduce the pulse with as great a magnitude as the normal part. These phenomena were similar to that observed by Haruo Okino and colleagues.[23] Thus, our model simulated realistic haptic feedback reflecting the dynamic physical behavior of both a normal and a sclerotic aorta wall.

The developed model had 1,651 vertices, which provided sufficient visual quality to represent the 3D shape of an aortic arch. In this case, the calculation time was 0.08 ms for force feedback and 0.5 ms for deformation. These times confirmed that the proposed calculation methods achieved a sufficient refresh rate to handle deformable virtual media with autonomous beating.

User tests

As we explained, the system's role was to support the communication of knowledge on aorta bioelasticity. We categorized this communication in three separate procedures and planned three user studies to test how well the system supported this communication, basing each experiment on each of the following hypotheses:

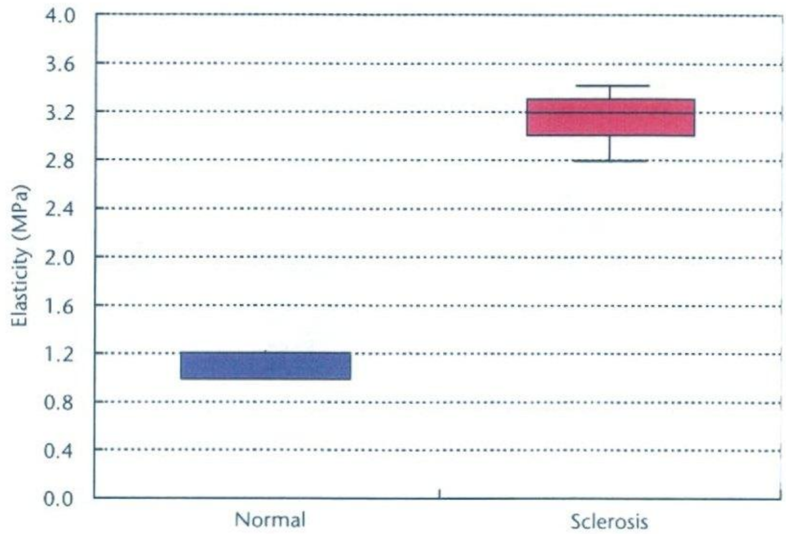

Figure 8. Interactive modeling results of normal elasticity and the threshold elasticity that should be regarded as sclerotic. The box plot indicates 25 percent (minimum) and 75 percent (maximum) of the data. This demonstrates that skilled surgeons are able to recognize key aorta palpation bioelasticity and also show their knowledge on bioelasticity in aorta palpation.

- *Elasticity modeling.* If experts knew the aorta's correct tissue elasticity during palpation and the system provided a valid elasticity-modeling environment, we could set up the virtual aorta with identical given elasticity.
- *Elasticity recognition.* If haptic interaction with the virtual media effectively supported communication on bioelasticity, trainees would be able to recognize the given elasticity more easily than with other training methods.
- *Learning elasticity.* If the system supported instruction of a specific bioelasticity, trainees would be able to learn the given elasticity through continuous repetition of the palpation procedure.

We focused on two elasticity conditions that were considered key in intraoperative aorta palpation: normal tissue elasticity and the threshold elasticity that's regarded as sclerotic. Cardiovascular surgeons have to learn both elasticity conditions to identify the sclerotic region and determine the overall surgical strategy. In the next three sections, we describe the results of the user study.

Elasticity modeling

First, we examined the capability of the system to carry out elasticity modeling of the virtual aorta, working with eight skilled surgeons from the Department of Cardiovascular Surgery at Kyoto University Hospital. We prepared 20 aorta models with the same 3D shape (shown in Figure 4) but different levels of stiffness. We set the uniform elasticity of each model by changing the input parameter of Young's modulus, which varied from 0.2 MPa to 4.0 MPa. The Poisson's ratio was set as 0.48. In advance of the experiment, we allowed the surgeons a few minutes of practice time during which they attempted the palpation procedure at leisure to accustom themselves to the virtual environment.

For the study itself, the surgeons conducted a normal palpation procedure on the 3D virtual aorta. If the physical behavior and reaction force differed from their expectation of how a normal aorta should have behaved, we changed the model elasticity accordingly. They repeatedly palpated the models and selected the one that most realistically simulated the elasticity of a normal aorta. The same procedure was used to determine the threshold elasticity that should have indicated sclerosis in real surgery. We randomized the order in which the surgeons tested the different models. The same palpation point on the model was used for all surgeons.

Figure 8 shows the statistical results for the models that were selected for normal and sclerotic elasticity conditions. The left-hand graph shows there were only two different models, 1.0 MPa and 1.2 MPa, which the surgeons deemed to correspond to their experience of a normal aorta. Specifically, five surgeons selected the 1.0-MPa model; three chose the 1.2-MPa model. Next, the right-hand graph in Figure 8 shows the results of selection for the sclerotic aorta. The graph suggests that anything over 3.0 MPa corresponded to sclerosis, according to the experience of the surgeons. These results lead us to the following insights:

- A virtual aorta with a Young's modulus between 1.0 MPa and 1.2 MPa effectively displays the physical behavior of a normal aorta.
- A virtual aorta having a Young's modulus of over 3.0 MPa simulates sclerotic status.
- All skilled surgeons recognize the absolute elasticity of normal and sclerotic conditions by touch. This means that elasticity is the most important information to communicate when trainees try to master the palpation of an aorta.

The surgeons who evaluated our system reported that manipulating the virtual model using the two Phantom devices was comparable to the experience of real surgery. Also, they stated that they experienced a realistic reaction force following adjustment of the model's physical parameters. In addition, a sufficiently small disagreement arose among the surgeons in choosing the models that best represented normal and sclerotic conditions of the aorta. These results indicate that our system enabled virtual palpation that effectively mirrored the real-life procedure.

Elasticity recognition

As shown in the first experiment, the ability to recognize the elasticity of normal and sclerotic aortas is important. In our second experiment, we aimed to confirm that haptic interaction with a deformable media was useful for bioelasticity training. We initiated a study with 18 medical students who hadn't experienced palpation of a real aorta and examined their ability to recognize different elasticity conditions.

Ten of the virtual aorta models used in the previous experiment were again prepared and the students performed virtual palpation in the same manner. Again the elasticity ranged from 0.2 MPa to 2.0 MPa. Some time was given for the students to become accustomed to manipulation and the manner of touching the model in virtual space. Then, each student was asked to select the model, which they thought best represented a real-life normal aorta. We prepared the students for making their selection under the following conditions.

Condition 1: No information. The medical students had only experienced the elasticity of a cadaver's aorta during their medical training and had not received any specific instruction on aorta elasticity prior to starting the experiment. Because the elasticity of a cadaver is totally different from that of a living body, they had no experience of an in vivo aorta and, in selecting from among our models, had to imagine what a real aorta would feel like.

Condition 2: Verbal information. The students underwent instruction from cardiovascular surgeons who described the physical characteristics of a normal aorta using both brief explanation and rubber hoses as a physical representation of aorta elasticity. This technique is a conventional teaching method.

Condition 3: Haptic instruction. The medical students were given 1 minute to become familiar with the elasticity of a normal aorta by carrying out virtual palpation on our developed system. The 1.0 MPa value was specified as the Young's modulus of this "normal" virtual aorta.

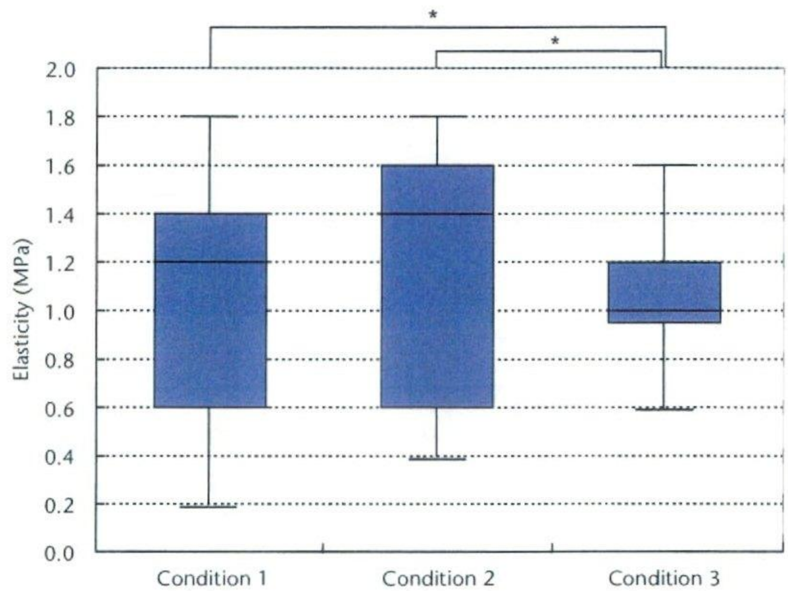

Figure 9. Statistical results of elasticity recognition of a 1.0-MPa normal aorta model in three cases: conventional instruction (condition 1 or 2) and simulator-based instruction (condition 3). (The asterisks indicate significant statistical difference between the two data values.)

Figure 9 illustrates the statistical results for the elasticity of the models that the students selected. The statistical analysis (F-test) result shows significant difference between the conventional means of instruction (condition 1 and condition 2) and simulator-based instruction (condition 3). The distribution of the graph at condition 2 still shows a large spread. This result shows that verbal communication alone isn't an effective means for students to learn the elasticity of a specific aorta condition, because students have an existing expectation of the elasticity that can't be altered simply by hearing what it should feel like. The graph of condition 3 is close to a normal distribution, and more than 80 percent of the students selected models with elasticity between 0.8 MPa and 1.2 MPa. This result demonstrates that haptic interaction using our system is an effective method for enabling students to recognize the normal stiffness of the virtual aorta model. Furthermore, the Young's modulus of 1.0 MPa had been configured by expert surgeons in the previous experiment, meaning that the students effectively experienced the elastic characteristics of an in vivo normal aorta through virtual palpation. We only conducted the second experiment employing the normal aorta because verbal representation isn't generally used to describe a sclerotic aorta in clinical work.

Learning elasticity

In this third, final experiment, we tested the effectiveness of learning elasticity through virtu-

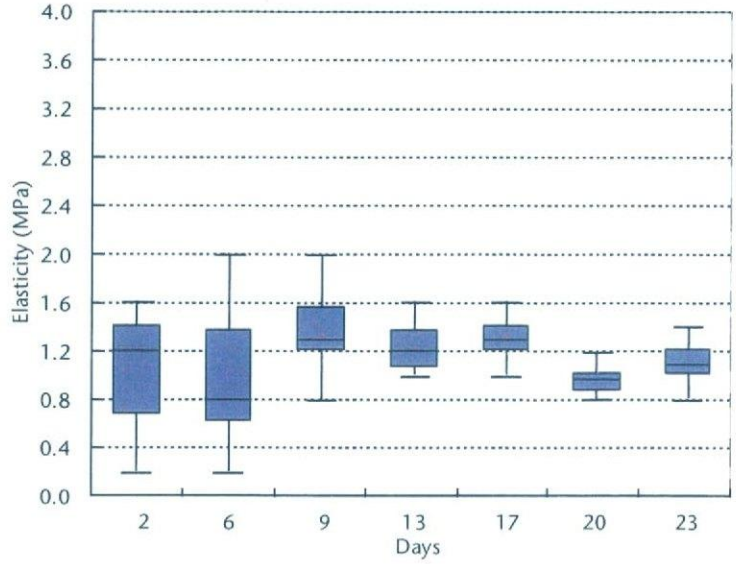

Figure 10. Virtual palpation learning curve for the normal model. The target was 1.0 MPa. The spread narrowed and the median selection approached 1.0 MPa over time.

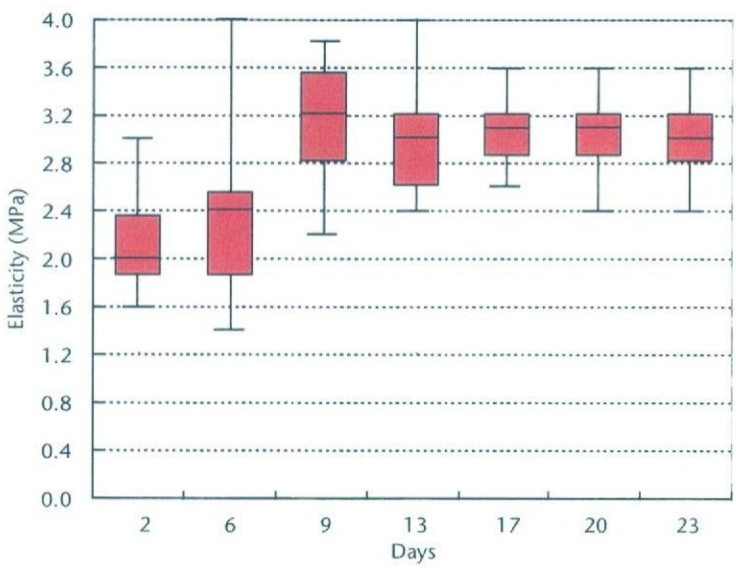

Figure 11. Virtual palpation learning curve for the sclerotic model. The target was 3.0 MPa. The spread narrowed and the median approached the target over time. Compared to Figure 10, each trial features a greater spread of selections.

al palpation. The second experiment had demonstrated that haptic instruction is an efficient means of enabling elasticity recognition, but to master palpation, students must memorize the critical elasticity they encounter during the procedure. Therefore, our study needed to further examine whether students were able to retain their knowledge of elasticity. In this last experiment, we aimed to provide students with a learning curve, in the form of a month-long course of training. We carried out the simulator-based learning based on the following conditions:

- The participants were 10 students who hadn't previously experienced a real aorta through touch.
- For each participant, seven trials were conducted, occurring approximately twice a week. The total experimental period was 23 days.
- Each trial consisted of two steps: testing and learning. Participants completed both steps at every trial.
- Test stage: Participants were asked to select the aorta models that they believed to be normal or sclerotic, from 20 aorta models with Young's modulus between 0.2 MPa and 4.0 MPa, based on their current bioelasticity knowledge.
- Learning stage: The correct normal (1.0 MPa) and sclerotic (3.0 MPa) aorta models were revealed. Examinees were given a few minutes to try to learn the elasticity of the models through virtual palpation.
- The palpation point on the aorta model was fixed throughout the experiment.

Figure 10 shows the selection data over the course of the third experiment in which the student participants attempted to choose the normal aorta. The spread of the participants' selections clearly narrowed over time, and the median eventually approached 1.0 MPa. Our statistical analysis (T-test) reveals a significant difference in the spread between the first and third trials, and the second and third trials. These graphs demonstrate that several separate training opportunities effectively contribute to learning the stiffness characteristics of the normal aorta.

Figure 11, which shows the selection data for the sclerotic condition, suggests that haptic instruction using the developed system is effective. However, there is a wider spread in the selections, compared to the learning curve in Figure 10. This tendency is consistent with what is known about human perception, in that human haptic sensitivity to relative physical behavior is proportional to the logarithm of absolute stiffness.

Final remarks

In evaluating the results of our experiments, we discuss how the efficacy of realistic VR-based palpation might be further improved. First, to achieve a real-time refresh rate, we simplified the physical behavior of an in vivo aorta by ignoring some essential functions. We didn't consider the effects of local pressure or blood flow, and simulated continuous autonomous beating with discrete time-series blood-pressure data. For noncomplex 3D aorta models, the blood pressure applied to the internal walls was assumed to be constant and independent of local position. The advantage of this simplification was that it aided fast calculation for valid haptic feedback and let us reproduce key soft-tissue behavior (for example, pulsation and elasticity) in virtual palpation. Our model achieved a refresh rate of more than 1,000 Hz in the reaction force calculation owing to our simplification of boundary conditions and inverse matrix calculation.

Another simplification was to reproduce the dynamic force of autonomous beating using a static FEM model. The variance in elasticity between the model and real life was small, and the surgeons who evaluated our system agreed that it demonstrated realistic force feedback and graphical deformation for the palpation procedure.

Although VR-based surgical simulators provide an effective training environment in clinical training, the representation and validation of specific bioelasticity behavior remains a problem. Both our proposed bioelasticity communication support environment and the quantified knowledge gained during our study will be useful indices for the future development of haptic anatomical models.

The approach we followed is potentially applicable to other virtual organ models that require a multiphysics simulation. We suggest that more detailed modeling, especially focused on a number of specific diseases and morbid stages, will be carried out as future work. This work will contribute to the compilation of practical instruction courseware. **MM**

Acknowledgment

This research was supported by a Grant-in-Aid for Scientific Research (S) (16100001) and Young Scientists (A) (16680024) from the Ministry of Education, Culture, Sports, Science, and Technology, Japan.

References

1. P.J. Gorman, A.H. Meier, and M. Krummel, "Computer-Assisted Training and Learning in Surgery," *Computer Aided Surgery*, vol. 5, 2000, pp. 120-127.
2. U. Kuhnapfel, H.K. Cakmak, and H. Mass, "Endoscopic Surgery Training Using Virtual Reality and Deformable Tissue Simulation," *Computer Graphics*, vol. 24, no. 5, 2000, pp. 671-682.
3. C. Wagner, M.A. Schill, and R. Manner, "Collision Detection and Tissue Modeling in a VR Simulator for Eye Surgery," *Proc. Workshop on Virtual Environments*, 2002, ACM Int'l Conf. Proc. Series, ACM Press, pp. 27-36.
4. S. Baillie et al., "Validation of a Bovine Rectal Palpation Simulator for Training Veterinary Students," *Proc. Medicine Meets Virtual Reality Conf.* (MMVR), 2005, IOS Press, pp. 33-36.
5. T. Tokuyasu et al., "Mechanical Modeling of a Beating Heart for Cardiac Palpation Training System," *Int'l J. Robotics Soc. Japan*, vol. 17, no. 6, 2003, pp. 463-479.
6. M. Nakao et al., "Haptic Reproduction and Real Time Visualization of a Beating Heart for Cardiovascular Surgery Simulation," *Int'l J. Medical Informatics*, vol. 68, issue 1-3, 2002, pp. 153-161.
7. Y. Kuroda et al., "Interaction Model between Elastic Objects for Haptic Feedback Considering Collisions of Soft Tissue," *Computer Methods and Programs in Biomedicine*, vol. 80, no. 3, 2005, pp. 216-224.
8. D. Braff and A. Witkin, "Physically Based Modeling: Principles and Practice," *ACM Siggraph Course Notes*, ACM Press, 1997.
9. M. Bro-Nielsen and S. Cotin, "Real-Time Volumetric Deformable Models for Surgery Simulation Using Finite Elements and Condensation," *Eurographics Computer Graphics Forum*, vol. 15, no. 3, 1996, pp. 57-66.
10. S. Cotin, H. Delingette, and N. Ayache, "A Hybrid Elastic Model Allowing Real-Time Cutting, Deformations, and Force Feedback for Surgery Training and Simulation," *The Visual Computer*, vol. 16, no. 7, 2000, pp. 437-452.
11. E. Gladilin, *Biomechanical Modeling of Soft Tissue and Facial Expressions for Craniofacial Surgery Planning*, doctoral dissertation, Mathematics Dept., Free University Berlin, 2002.
12. R. Balaniuk and K. Salisbury, "Dynamic Simulation of Deformable Objects Using the Long Elements Method," *Proc. 10th Symp. Haptic Interfaces for Virtual Environments and Teleoperator Systems*, IEEE CS Press, 2002, pp. 58-65.
13. J. Berkley et al., "Banded Matrix Approach to Finite Element Modeling for Soft Tissue Simulation," *Virtual Reality Research Development and Application*, vol. 4, 1999, pp. 203-212.
14. K. Hirota and T. Kaneko, "Haptic Representation of Elastic Object," *Presence*, vol. 10, no. 5, 2001, pp. 525-536.

15. S. Capell et al., "A Multiresolution Framework for Dynamic Deformations," *Proc. ACM Siggraph Symp. Computer Animation*, 2002, pp. 41-47.
16. N.E. Seymour, "Virtual Reality Training Improves Operating Room Performance: Results of a Randomized Doubleblinded Study," *Annals of Surgery*, vol. 236, no. 4, 2002, pp. 458-463.
17. T.P. Grantcharov et al., "Randomized Clinical Trial of Virtual Reality Simulation for Laparoscopic Skills Training," *British J. Surgery*, vol. 91, 2004, pp. 146-150.
18. R. Kikuuwe and T. Yoshikawa, "Haptic Display Device with Fingertip Presser for Motion/Force Teaching to Human," *Proc. IEEE Int'l Conf. Robotics and Automation*, 2001, pp. 868-873.
19. S. Saga, N. Kawakami, and S. Tachi, "Haptic Teaching Using Opposite Force," poster presentation and demonstration, *Proc. World Haptics Conf.*, IEEE CS Press, 2005.
20. M.J. Ackermann, "The Visible Human Project: A Resource for Anatomical Visualization," *Proc. Medical Informatics* (Medinfo), 1998, pp. 1030-1032.
21. C.B. Zilles and J.K. Salisbury, "A Constraint-Based God-Object Method for Haptic Display," *Proc. IEEE/RSJ Int'l Conf. Intelligent Robots and Systems* (IROS), vol. 3, IEEE CS Press, 1995, pp. 141-151.
22. D. Ruspini, K. Kolarov, and O. Khatib, "The Haptic Display of Complex Graphical Environments," *Proc. ACM Siggraph*, ACM Press, 1997, pp. 345-352.
23. H. Okino, H. Matsuo, and M. Sugawara, *Shinzou Kekkankei no Rikigaku to Kiso Keisoku* [Cardiovascular System Mechanics and Basic Measurements], Kodansha Ltd., 1980, pp. 188-189 (in Japanese).

Megumi Nakao is an assistant professor in biomedical imaging and informatics at the Graduate School of Information Science, Nara Institute of Science and Technology. His research interests include medical virtual reality, computer graphics and haptics, physics-based modeling and biomedical engineering. Nakao has a PhD in informatics from Kyoto University.

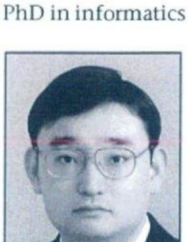

Tomohiro Kuroda is the vice-director in the Department of Medical Informatics at Kyoto University Hospital. He also holds a docent position at Osaka Sangyo University and a visiting-professor position at the University of Oulu. His research interests include the human interface, virtual/augmented reality, wearable computing, and medical and assistive informatics. Kuroda has a PhD in information science from the Nara Institute of Science and Technology.

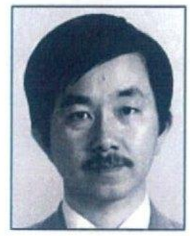

Masaru Komori is a professor of computational biomedicine at the Shiga University of Medical Science. His research interests are virtual reality applications in the medical field, medical imaging, and medical informatics. Komori has a PhD in electrical engineering from Kyoto University.

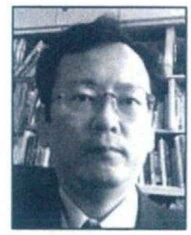

Hiroshi Oyama is a professor of clinical bioinformatics engineering, and an adjunct professor of medical informatics and economics at the University of Tokyo. His research interests include biomedical computing and modeling and their application to virtual reality, telemedicine, surgical simulation, palliative medical systems, and ubiquitous medicine. Oyama has a PhD in medicine from the University of Tsukuba.

Kotaro Minato is a professor of biomedical imaging and informatics at the Graduate School of Information Science, Nara Institute of Science and Technology. His research interests include medical informatics, medical imaging, and biomedical engineering. Minato has a PhD in electrical engineering from Kyoto University.

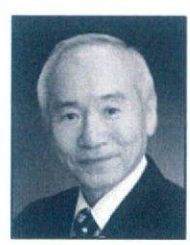

Takashi Takahashi is the president of the Kyoto College of Medical Technology and an emeritus professor at Kyoto University. His research interests include medical informatics, medical virtual reality, and medical engineering. Takahashi has a PhD in electronic engineering from Osaka University.

Readers may contact Megumi Nakao at the Nara Institute of Science and Technology, Graduate School of Information Science, 8916-5, Takayama, Ikoma, Nara, 630-0192, Japan; meg@is.naist.jp.

A Computational Method for Identifying Medical Complications based on Hospital Information System Data

Nobuo Shinohara[1], Hiroshi Oyama[1], Shiro Matsuya[1], Kazuhiko Ohe[2]

[1] Clinical Bioinformatics Research Unit, Graduate School of Medicine, The University of Tokyo,

2 Department of Medical Informatics and Economics, Graduate School of Medicine, The University of Tokyo, T Tokyo, Japan

Email: nsinohara-tky@umin.ac.jp

Abstract: This study introduces an objective method of identifying medical complications based only on Hospital Information System (HIS) data. To identify medical complications, we established a rule, prepared HIS data, and applied the rule to the data. If an accurate count of medical complications can be made, this could become one clinical indicator for evaluating the quality of risk management in clinical care.

Keywords: Clinical Indicator, Medical Complication, Hospital Information System

1. Background

One of the important tasks in the risk management of clinical care is to minimize the rate of medical complications. The number of medical complications should be a major clinical indicator for evaluating the quality of risk management in clinical care. We can determine the quality of risk management by comparing the indicator relatively and absolutely. However, there is no objective method for obtaining accurate numbers of medical complication cases. Here, we developed a method to calculate these numbers using only data stored in the Hospital Information System (HIS).

2. Objective

We chose one medical complication—shock symptom with intravenous application of contrast media during c omputed tomography (CT) examination. Severe grade of this complication occurs in 0.04% cases with non-io nic contrast media[1)]. This study aimed to construct a m ethod for extracting such medical complication data us ing only HIS data.

3. Methods

This study was conducted in three steps [Figure 1 (1)–(3)]. First, we established a heuristic rule for identifying patients who may have suffered shock symptoms after interviewing one radiologist and one emergency physician (1). Next, we prepared HIS data to test the ability of the rule to identify patients who may have had the complication (2). HIS consists of two types of data: clinical data and accounting data. We decided to use accounting system data first and to use clinical data if necessary. Lastly, we identified patients who may have had the complication by applying the rule to the data (3). Then, we checked whether the patients really had the complication by surveying their clinical records, thereby evaluating the rule.

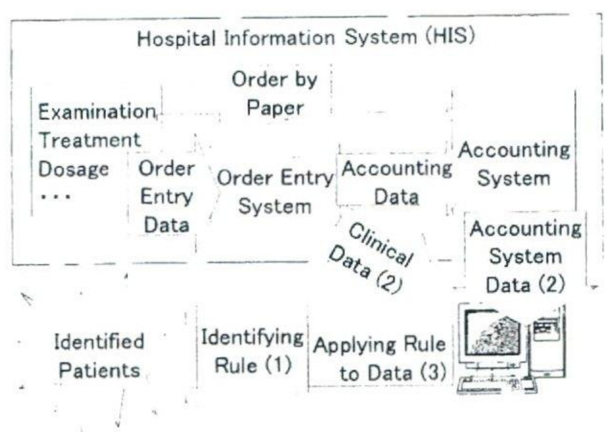

Figure 1. Overview of this study

4. Results

Identifying rule

The identifying rule is shown in Figure 2.

```
Patients {
    who {
        are given an antihistamine or steroid by I.V. or
        at the time of CT examination without any
        orders − (1)
    } and {
        use oxygen
    } and {
        have no surgery
    } on the day of CT examination with contrast media
} and {
    who are not given an antihistamine or steroid three
    days before or after the day of the CT examination
}
```

Figure 2. Identifying rule

Applying the identifying rule to data

First, we applied the rule to data stored in The University of Tokyo Hospital's accounting system between 1 April 2003 and 31 March 2004. We had to alter the rule so that it applied to accounting data only. For example, we need to ignore "without any orders" from line (1) in Figure 2 and interpret the line as "are given an antihistamine or steroid by I.V. or at the time of CT examination" because we cannot recognize that the antihistamine or steroid is administered "with some orders" or "without any orders" from the accounting data. The number of identified patients who may have suffered the complication using only accounting data is shown in Table 1.

Table 1. Using only accounting data

Period of time	1 Apr. 2003–31 Mar. 2004
Total number of CT examinations with contrast media	14,255
Number of patients who may have suffered the complication	5
Actual number of patients who suffered the complication	3

Next, we added data stored in the inpatient injection or der entry system to recognize the administration of an antihistamine or steroid as "with some orders" or "with out any orders" and applied the rule strictly. The result of applying the rule to the HIS data is shown in Table 2 . The number of patients who may have suffered compl ications decreased from five to four.

Table 2. After using the inpatient injection order entry system data

Period of time	1 Apr. 2003–31 Mar. 2004
Total number of CT examinations with contrast media	14,255
Number of patients who may have suffered the complication	4
Actual number of patients who suffered the complication	3

4. Discussion and Conclusion

Since accounting rules are the same throughout Japan, we should be able to apply the method presented here to data in the accounting systems of other hospitals easily. This is a great advantage of using accounting data first.

As shown in Table 2, one patient was misidentified as suffering complications. The cause of the misidentification was the administration of a steroid to prevent shock symptoms. This type of error is difficult to avoid using accounting data only because the system does not record time. The system records the date only. Inputting additional clinical data would be able to resolve this problem.

To use the number of patients who may have suffered complications as a clinical indicator, we must first obtain the actual number of such patients and evaluate the precision and recall of the identifying rule. This will be the next stage of our study.

In the present study, we presented a computational met hod for identifying medical complications based only o n HIS data and successfully identified patients who suf fered medical complications.

References

[1] Katayama H, Yamaguchi K, Kozuka T, Takashima T, Seez P, Matsuura K. Adverse Reactions to Ionic and Nonionic Contrast Media. Radiology. 1990; 175: 621–628.

Address correspondence to:

Nobuo Shinohara
Clinical Bioinformatics Research Unit
Graduate School of Medicine, The University of Tokyo
7-3-1 Hongo, Bunkyo-ku, Tokyo 113-8655, Japan
E-mail: nsinohara-tky@umin.ac.jp

A data mining method for discovering causal relationships between harmful chemicals and clinical symptoms

Yuichi Katsumura[1], Nobuo Shinohara[2], Shinya Matsumoto[2], Tomoaki Imamura[3], Hiroshi Oyama[2]

[1] School of Health Sciences and Nursing, School of Medicine, The University of Tokyo
[2] Clinical Bioinformatics Research Unit, Graduate School of Medicine, The University of Tokyo
3 Department of Planning, Information and Management, The University of Tokyo
Japan, ykatsumura-tky@umin.ac.jp

Abstract: Analyzing the compound effects of harmful chemicals is difficult using statistical methods because massive computational power is required. We examined whether hypotheses could be generated using an association rule to examine the relationships between the blood concentrations of three harmful chemicals (A, B, and C) and clinical symptoms, after using categorization to reduce the volume of data. The application of an association rule mining algorithm revealed a relationship between (a) dermatological symptoms and high concentrations of chemicals A and B and (b) ophthalmological symptoms and the concentration of chemical A. Our study demonstrates that data mining of categorized data can be used to generate new hypotheses about the relationships between harmful chemicals in blood and clinical symptoms.

Keywords—Data mining, Association rules

I. INTRODUCTION

Harmful chemicals cause a variety of clinical symptoms. Methods to elucidate the relationships between harmful chemicals and clinical symptoms have not been established, and the analysis of the compound effects of harmful chemicals is particularly difficult using statistical methods because massive computational power is required. By contrast, data mining can be used to analyze large volumes of clinical data [1], because this method can handle many variables simultaneously, which is difficult to do using statistical methods. However, data mining is essentially an exploratory analytical method and cannot be used to test hypotheses. This is particularly problematic for the interpretation of clinical data, which requires expert analysis [2]. Dimensional reduction and data reduction are crucial for efficiently obtaining good rules of association [3]. In this study, we demonstrate that the application of a novel method of data categorization to reduce the computational power required for analysis can be used to generate hypotheses about the relations between harmful chemical concentrations and clinical symptoms.

II. METHOD

We analyzed data collected over a period of three years from 795 patients who were suspected of having been exposed to harmful chemicals. The data included the presence or absence of different clinical symptoms (dermatological, dental, and ophthalmological) and the blood concentrations of three harmful chemicals (A, B, and C). The results of clinical and laboratory examinations were included in the analysis as 241 individual items (Table 1). To eliminate dignity weighting, we only covered the data of each people's oldest year to become one-person one record, and theni t became 381 records.

Given the large number of variables to be analyzed and the requirement that symptoms be analyzed as objective and explanatory variables, we applied an association rule mining algorithm using Teradata Warehouse Miner (NCR Japan, Ltd).

Table 1. Examination number of items

blood chemistry	52
Internal medicine	55
Dermatology	21
Dentistry	108
Ophthalmology	5
Total	241

To reduce the computational calculations, we categorized the data as follows. First, we only included data that were anomalous, because we focused on the relationship between anomalous symptoms and harmful chemical concentrations. Second, in order to reduce the amount of calculation, we converted three variables that described the blood concentrations of chemicals A, B, and C into a single variable by combining the high and low concentrations of each chemical; we thus considered the compound effects of each chemical. To categorize a concentration as high or low, we used upper and lower tertile, respectively. We then created a data set for all patients [personal identification number (ID), anomalous symptoms, and combination of harmful chemicals] and applied the association rule mining algorithm. In order to find whether there is any internal-organs singularity with each substance, rules contain the combination of three kinds of symptom were considered. To evaluate the association rules that were obtained, we use the confidence and support values and the lift.

Even if a support value is especially low in a medical field, it is thought that the rule is satisfactory. However, since the information whether possession of left item has influenced the likelihood of possession of right item was not known only with the confidence, the lift which measures the difference between actual confidence and expected confidence was used. For example, when a lift is 1.5, it means that it is higher than a rate 50% when the rate which owns left item and right item sees on the whole. In order to remove the combination generated by chance, we removed the rules if support was 0.013 or less so that the number of people with which a rule was applied became five or more persons.

III. RESULTS

In Tables 2, we present the results of applying the association rule mining algorithm and the rules with a confidence greater than 0.5 and a lift greater than 1.2. The values in Tables 2 describe the associations for t he items in the first two columns. Table 2 contains asso ciation rules for two items (chemical concentrations an d a single symptom; hereafter referred to as a 1–1 asso ciation).

Table 2. Main association rules

ITEM (LEFT)	ITEM (RIGHT)	LSUPPORT	RSUPPORT	SUPPORT	CONFIDENCE	LIFT	ZSCORE
A_B_C (High_High_High)	past history of pig mentation	0.0866	0.4514	0.0551	0.6364	1.4098	1.6133
A_B_C (High_High_High)	past history of anc eform eruptions	0.0866	0.6063	0.0656	0.7577	1.2496	1.1471
A_B_C (High_High_Low)	past history of pig mentation	0.0236	0.4514	0.0236	1.0000	2.2151	2.4624
A_B_C (High_High_Low)	past history of anc eform eruptions	0.0236	0.6063	0.0236	1.0000	1.6494	1.5278
A_B_C (High_High_Low)	arthralgia	0.0236	0.6378	0.0184	0.7777	1.2194	0.5296
A_B_C (Low_High_Low)	abdominal pain	0.0577	0.3097	0.0289	0.5000	1.6144	1.6183
A_B_C (Low_High_Low)	arthralgia	0.0577	0.6378	0.0472	0.8182	1.2828	1.0793
A_B_C (Low_High_Low)	constipation	0.0577	0.3858	0.0289	0.5000	1.2959	0.8719
A_B_C (Low_High_Low)	cough	0.0577	0.4121	0.0289	0.5000	1.2134	0.6503
A_B_C (Low_Low_High)	abdominal pain	0.0210	0.3097	0.0131	0.6248	2.0172	1.6066
A_B_C (Low_Low_High)	general fatigue	0.0210	0.6509	0.0210	1.0000	1.5363	1.2323
A_B_C (Low_Low_High)	headache	0.0210	0.5722	0.0158	0.7500	1.3108	0.6690
A_B_C (Low_Low_Low)	diarrhea	0.0551	0.3255	0.0315	0.5715	1.7559	1.9942

The results of our analysis indicated that, whe n the concentrations of chemicals A and B were l ow, patients presented with diarrhea, headache, and general fatigue more often than with other sympt oms. High concentrations of the harmful chemicals A and B were associated with unique symptom s, such as a past history of pigmentation, a past h istory of anceform eruptions.

IV. DISCUSSION AND CONCLUSION

In this study, we used a novel method of data categorization followed by data mining to analyze the relationship between the blood concentrations of harmful chemicals and various clinical symptoms. This approach generated several hypotheses. The symptoms presented by the patients included in this study were suspected to have been caused by exposure to chemicals A and B. Indeed, the associations between clinical symptoms and the concentrations of chemicals A and B have been described in numerous reports. Our method of analysis also revealed such relationships, for example, that between a past history of pigmentation and high concentrations of chemicals A and B (see Table 2). In contrast, the hypothesis discovered newly in this study needs to be inquired by the medical expert.

One limitation of our method is the manner in which numeric values are considered. We categorized the concentrations of harmful chemicals into two categories (high and low) according to tertile, but superior measurement criteria could be used, such as numeric association rules [4]. Another limitation is the sample size. To elucidate the compound effects of the harmful chemicals, we categorized participants into eight groups, and this resulted in an insufficient number of patients within each group. For this reason, the z-score might have been underestimated.

In conclusion, the method used in this study to reduce the computational power required for data analysis can create new hypotheses about the relationship between blood concentrations of harmful chemicals and clinical symptoms. It is thought that it can not generalize to the general talk of a harmful chemistry substance from this data, since those who are conjectured not to have taken in the harmful chemistry substance but are shown similar symptoms exist. In next study, we are due to search for the relevance of an exact antineoplastic drug, the concentration in blood of the metabolism product, and side effects (agranulocytosis, diarrhea, a feeling of fatigue, etc.).

REFERENCES

[1] Lavrac N. Selected techniques for data mining in m edicine. Artif Intell Med 1999, 16: 3-23

[2] John F. Roddick, Peter Fule, Warwick J. Graco Exploratory Medical Knowledge Discovery: Exper iences and Issues. ACM SIGKDD Explorations Ne wsletter, July 2003, 5(1): 94-99

[3] Nam Huyn. Data Analysis and Mining in the Life Sciences. SIGMOD Record, September 2001, 30(3): 76-85

[4] Fukuda T, Morimoto Y, Morishita S, and Toku yama T. Mining-optimized association rules for nu meric attributes. Journal of Computer and System Sciences, 1999, 58(1): 1–15